Protease-mediated enhancement of severe acute respiratory syndrome coronavirus infection

Shutoku Matsuyama*, Makoto Ujike*, Shigeru Morikawa†, Masato Tashiro*, and Fumihiro Taguchi*‡

Division of Respiratory Viral Diseases and SARS, *Department of Virology III, Special Pathogens Laboratory, †Department of Virology I, National Institute of Infectious Diseases, Murayama Branch, Gakuen 4-7-1, Musashi-Murayama, Tokyo 208-0011, Japan

Edited by Peter Palese, Mount Sinai School of Medicine, New York, NY, and approved July 19, 2005 (received for review April 19, 2005)

A unique coronavirus severe acute respiratory syndrome-coronavirus (SARS-CoV) was revealed to be a causative agent of a life-threatening SARS. Although this virus grows in a variety of tissues that express its receptor, the mechanism of the severe respiratory illness caused by this virus is not well understood. Here, we report a possible mechanism for the extensive damage seen in the major target organs for this disease. A recent study of the cell entry mechanism of SARS-CoV reveals that it takes an endosomal pathway. We found that proteases such as trypsin and thermolysin enabled SARS-CoV adsorbed onto the cell surface to enter cells directly from that site. This finding shows that SARS-CoV has the potential to take two distinct pathways for cell entry, depending on the presence of proteases in the environment. Moreover, the protease-mediated entry facilitated a 100- to 1,000-fold higher efficient infection than did the endosomal pathway used in the absence of proteases. These results suggest that the proteases produced in the lungs by inflammatory cells are responsible for high multiplication of SARS-CoV, which results in severe lung tissue damage. Likewise, elastase, a major protease produced in the lungs during inflammation, also enhanced SARS-CoV infection in cultured cells.

cell entry | protease | spike protein | SARS

Severe acute respiratory syndrome (SARS) is caused by a SARS-associated coronavirus (SARS-CoV), a newly emergent member in a family of Coronaviridae (1–6). Unlike other human coronaviruses, SARS-CoV causes a fatal respiratory disease in humans (1–6). Coronavirus is an enveloped virus with a positive-stranded large genomic RNA with ≈30 kb (7). Spikes exist on the virion surface and resemble solar corona, each of which is composed of a trimer of the spike (S) protein (7, 8). The S protein is a type I fusion protein of an approximate molecular weight of 180 kDa. The prototypical coronavirus mouse hepatitis virus enters into cells via the cell surface, although a variant isolated from persistent infection enters from an endosome, the low pH of which induces its fusion activity (9). However, the entry pathway of SARS-CoV appears to be distinct from that of the other coronaviruses. Simmons *et al.* (10) hypothesized that SARS-CoV enters cells by an endosomal pathway, and S protein is activated for fusion by trypsin-like protease in an acidic environment. This idea is based on the following two findings: (*i*) SARS-CoV infection can be blocked by lysosomotropic agents, and (*ii*) S protein expressed on cells is activated for fusion by trypsin. These results were obtained by studies using pseudotype retroviruses harboring SARS-CoV S protein on the envelope and those using S protein expressed on cells by expression vectors (10).

In the present study, we show that various proteases, as well as trypsin, are effective in inducing the fusion of SARS-CoV-infected VeroE6 cells. These proteases facilitated SARS-CoV entry from the cell surface, which indicates that SARS-CoV has the potential to enter cells via two different pathways, either an endosomal or a nonendosomal pathway, depending on the presence of proteases. More interestingly, SARS-CoV entry from cell surface mediated by protease resulted in >100-fold more efficient infection than entry through endosome. Elastase, a major protease produced during lung inflammation, also manifested this enhancing effect. These findings suggest that severe illness in the lungs and intestines is attributable to the proteases produced in these organs during an inflammatory response or in the presence of certain physiological conditions.

Materials and Methods

Cells and Viruses. VeroE6 cells were grown in DMEM (Nissui, Tokyo), supplemented with 5% FBS (GIBCO/BRL). The SARS-CoV Frankfurt 1 strain, kindly provided by J. Ziebuhr (University of Würzburg, Würzburg, Germany) (1), was propagated and assayed by using Vero E6 cells.

Proteases. Various proteases were dissolved in PBS (pH 7.2) and used at the indicated concentrations in DMEM containing 5% FCS. The proteases used in this study were trypsin (Sigma, T-8802), thermolysin (Sigma, P 1512), chymotrypsin (Sigma, C-3142), dispase (Roche, 1 276 921), papain (Worthington, 53J6521), proteinase K (Wako, Tokyo), collagenase (Sigma, C-5183), and elastase (Sigma, E-0258).

Plaque Assay. VeroE6 cells prepared in 24-well plates were inoculated with 50 μl of 10-fold serially diluted virus samples and incubated at 37°C for 1 h. Cells were then cultured with 0.5 ml per well of DMEM containing 1% FCS and 0.75% methyl cellulose (Sigma) for 2 d. Cells were fixed with 1 ml of 10% formaldehyde per well for at least 2 h. After removing the culture fluids, cells were irradiated overnight under a UV lamp and stained with crystal violet. Plaques produced by SARS-CoV were counted under light microscopy. Titration was done in duplicate and infectivity was displayed by plaque-forming units (pfu).

Western Blotting. S protein expressed in Vero E6 cells was analyzed by Western blotting. Preparation of cell lysates, SDS/PAGE, and electrical transfer of the protein onto a transfer membrane were described (11). S protein was detected with anti-S Ab, IMG-557 (Imgenex, San Diego) and horseradish peroxidase-conjugated anti-rabbit IgG Ab (anti-R-IgG, ALI3404, BioSource International, Camarillo, CA). The bands were visualized by using enhanced chemiluminescence reagents (ECL-plus, Amersham Pharmacia) on a LAS-1000 instrument (Fuji).

Real-Time PCR. VeroE6 cells in 96-well culture plates were treated with DMEM containing 1 μM bafilomycin (Baf; Sigma, B-1793) and 5% FCS (DMEM plus Baf) at 37°C for 30 min and then chilled on ice for 10 min. Approximately 10^4 pfu of virus in DMEM plus Baf were infected to 10^4 cells on ice; multiplicity of

This paper was submitted directly (Track II) to the PNAS office.

Abbreviations: SARS-CoV, severe acute respiratory syndrome-coronavirus; S, spike; pfu, plaque-forming unit; moi, multiplicity of infection; Baf, bafilomycin.

‡To whom correspondence should be addressed. E-mail: ftaguchi@nih.go.jp.

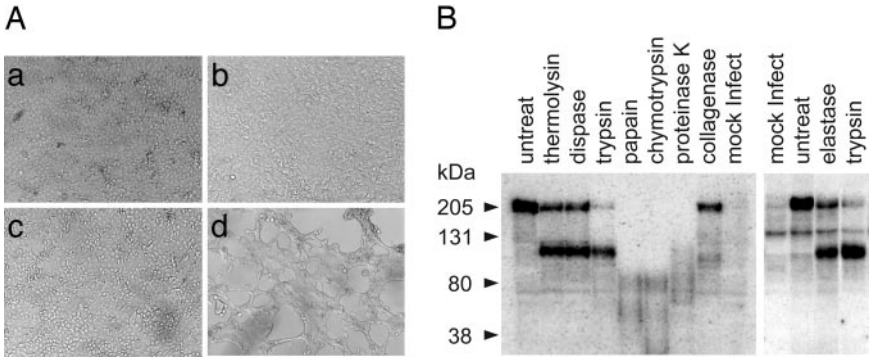

Fig. 1. Induction of cell-fusion and SARS-CoV S protein cleavage by proteases. (*A*) Syncytium formation after treatment with trypsin. VeroE6 cells cultured in 24-well plates were infected (*b* and *d*) or mock-infected (*a* and *c*) with the SARS-CoV Frankfurt 1 strain at moi = 0.5 and incubated at 37°C for 20 h. Cells were washed once with PBS and treated (*c* and *d*) or untreated (*a* and *b*) with 200 μg/ml trypsin for 5 min. Those cells were cultured for a further 4 h and observed by microscopy. (*B*) Western blot analysis of S protein treated with various proteases. Cells infected as described above were treated either with thermolysin (200 μg/ml), dispase (1 unit/ml), trypsin (200 μg/ml), papain (0.74 unit/ml), chymotrypsin (1 mg/ml), proteinase K (8 μg/ml) collagenase (200 μg/ml), or elastase (1 mg/ml), as described above. Soon after treatment, cells were lysed with lysing buffer, and S protein was analyzed by Western blot after SDS/PAGE. To detect the S protein (S2 fragment), mAb IMG-557 was used at a concentration of 5 μg/ml.

infection (moi) was at 1. After 30-min adsorption, the virus was removed, and infected cells were treated for 5 min with various concentrations of proteases in DMEM plus Baf that was prewarmed at room temperature. After protease was removed, cells were cultured in DMEM plus Baf at 37°C for 6 h. Vero E6 cell monolayers in 24-well plates were infected with 10 pfu of SARS-CoV (moi = 0.0001). After 30-min adsorption, cells were cultured in DMEM containing 5% FCS in the presence or in the absence of various proteases for 20 h. To isolate cellular RNA, 100 and 500 μl of isogen (Nippon Gene, Toyama, Japan) were added to each well of 96- and 24-well plates, respectively, together with 5 μg of yeast RNA as a carrier for 2-propanol precipitation. RNA was prepared according to the manufacturer's instructions and finally dissolved in 20 μl of diethyl pyrocarbonate-treated water. Real-time PCR was performed to estimate the amounts of mRNA9 in a final volume of 20 μl of 1× LightCycler RNA Master Mix (Roche Diagnostics) by using the RNA isolated as described above. For amplification of the fragment from mRNA9, we used 500 nM of a pair of oligonucleotides 5′-CTCGATCTCTTGTAGATCTG-3′ (SARS leader) and 5′-TCTAAGTTCCTCCTTGCCAT-3′ (SARS mRNA9 reverse). Amplified DNA from mRNA has 240 bases. With these primers, genomic RNA was not detected because the fragment to be amplified from genomic RNA would be ≈30 kb. For detection by hybridization, 200 nM each of the hybridization probes 5′-ACCAGAATGGAGGACGCAATGGGGCAAG-3′ (3′FITC labeled), 5′-CCAAAACAGCGCCGACCCCAAGGTTTAC-3′ (5′LCRed640 labeled) were used. PCR analysis was performed under the following conditions [reverse transcription: 61°C, 20 min; PCR, 95°C, 30 s (95°C, 5 s; 55°C, 15 s; 72°C, 10 s) ×45 cycles] with a LightCycler instrument (Roche Diagnostics). To measure the amounts of viruses that entered into cells, we infected cells with 10-fold stepwise diluted SARS-CoV from 10^6 to 10^2 pfu, and the amounts of mRNA9 were determined by real-time PCR. The amounts of virus that entered into cells after protease treatment were calculated from a calibration line obtained as above and shown as relative mRNA levels. When relative mRNA9 was higher than 10^6 pfu, samples were diluted and reexamined so that they were placed between 10^6 and 10^2 pfu.

Results

Activation of Cell Fusion and SARS-CoV S Protein Cleavage by Various Proteases. VeroE6 cells susceptible to SARS-CoV were infected with the Frankfurt-1 strain of SARS-CoV at a moi of 0.5, and those infected cells were treated with trypsin at 20 h after infection. Cell fusion was detected from 2 h after trypsin treatment (Fig. 1*Ad*). Fusion was also found after treatment with thermolysin or dispase (data not shown). Little or no fusion occurred after treatment with papain, chymotrypsin, proteinase K, or collagenase. S proteins in cells treated with proteases that induce fusion were cleaved approximately in the middle (Fig. 1*B*), a finding similar to that of Simmons *et al.* (10). In contrast, no apparent S2 band was detected in cells bearing S proteins treated with proteases that failed to induce fusion (Fig. 1*B*). These results showed that various proteases, including trypsin, activate the fusion activity of the SARS-CoV S protein by inducing its cleavage. Further, SARS-CoV infection was extensively inhibited by treatment of cells with Baf (Fig. 2*A*, no Baf vs. Baf without protease). These results suggest that SARS-CoV takes an endosomal pathway for its entry, and that S protein cleavage is important for fusogenicity, which is consistent with the conclusions of a previous report (10).

SARS-CoV Entry from Cell Surface Facilitated by Proteases. If the hypothesis proposed by Simmons *et al.* (10) is correct, we can make SARS-CoV enter cells directly from their surface by attaching the virus there and treating them with trypsin and other proteases that induce fusion. Treatment of VeroE6 cells with Baf at a concentration of 1 μM suppressed SARS-CoV infection via the endosomal pathway to $<1/100$, as shown in Fig. 2*A*. The cells treated with Baf were inoculated with SARS-CoV at a moi of 1 and incubated on ice for 30 min (adsorption on ice does not allow virus to enter cells). Then cells were treated with various proteases for 5 min at room temperature and incubated at 37°C for 6 h. Virus entry was estimated by the newly synthesized mRNA9 measured quantitatively by real-time PCR. A calibration curve of real-time PCR (Fig. 2*C*), showing the level of mRNA9 after infection with 10-fold diluted SARS-CoV, was used to estimate the amount of infected virus from the mRNA levels. As shown in Fig. 2*A*, thermolysin and trypsin, two proteases with fusion-inducing activity, extensively facilitated viral entry. In contrast, two proteases that did not induce fusion, papain and collagenase failed to do so. Treatment of cells with trypsin before virus infection did not facilitate viral entry (Fig. 2*B*), indicating that effects of trypsin on cells are not involved in this infection. Other proteases did not influence the SARS-CoV infection as trypsin, when treated before virus inoculation (data not shown). Protease treatment of SARS-CoV before infection did not enhance infectivity but reduced it by 10- to 100-fold (data

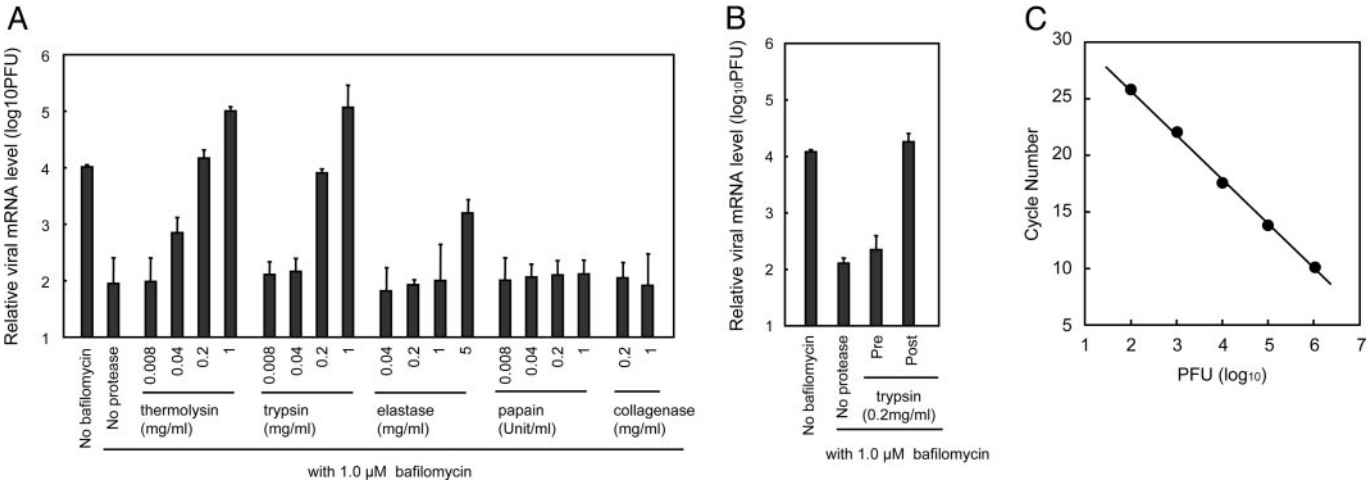

Fig. 2. Entry of SARS-CoV from cell surface facilitated by proteases. (*A*) Effect of proteases on SARS-CoV entry into VeroE6 cells treated with Baf. VeroE6 cells in 96-well plates were treated with Baf at a concentration of 1 μM at 37°C for 30 min, placed on ice and infected with SARS-CoV at moi = 1 for 30 min. Then, cells were treated with various concentrations of different proteases at room temperature for 5 min and cultured in the presence of Baf for a further 6 h. The amount of mRNA9 was measured quantitatively by real-time PCR. Cells untreated with Baf or those treated with Baf but untreated with protease were used as controls. The relative viral mRNA level is displayed by virus infectivity (pfu) calculated from a calibration line shown in *C*. (*B*) Cells treated with Baf at 37°C for 30 min were then treated with trypsin at room temperature for 5 min before (pre) or after (post) virus inoculation, and virus infection was estimated quantitatively by real-time PCR as described above. (*C*) Calibration in real-time PCR. VeroE6 cells in 94-well plates were infected with 10-fold step diluted viruses, and mRNA9 levels at 6 h after infection were estimated by real-time PCR. The relationship is shown between inoculated pfu (*x* axis) and cycles of real-time PCR to reach a positive level (amount of mRNA9) (*y* axis).

not shown). We believe these results demonstrate that SARS-CoV, when adsorbed onto the cell surface, fuse with the plasma membrane of its envelope with S protein, which is cleaved into S1 and S2 by proteases with fusion-inducing activity. This suggests a nonendosomal, direct entry of SARS-CoV into cells in the presence of proteases. Those findings also support the hypothesis drawn by Simmons *et al.* (10) that trypsin-like protease plays an important role in facilitating membrane fusion.

Enhancement of SARS-CoV Infection by Various Proteases. Treatment with a high concentration of thermolysin and trypsin augmented virus entry or replication by 10-fold or higher, as compared with the standard infection (Fig. 2*A*, e.g., compare bar 6 or bar 10 with bar 1 from the left). We then compared the replication kinetics of SARS-CoV in cells treated with Baf and a high concentration of trypsin with that of cells maintained without Baf or trypsin. The level of mRNA9 was always ≈10-fold higher in trypsin-treated cells at any given time during the early period of infection (Fig. 3). These data also imply that viral replication after entry via the cell surface proceeds ≈1 h ahead of that via the endosomal pathway, suggesting that the surface route is more efficient for rapid viral replication.

Because SARS-CoV replication was shown to be enhanced by trypsin treatment, we next assessed the efficiency of virus spread in the presence or absence of trypsin in a low moi, which mimics natural infection in target organs. Virus (10 pfu) were inoculated onto 10^5 confluent VeroE6 cells (moi = 0.0001), and the cells were incubated at 37°C for 20 h in the media with or without trypsin. The level of mRNA9 estimated quantitatively by real-time RT-PCR showed that virus replication was 100- to 1,000-fold higher when cells were cultured in the presence of trypsin, when compared with replication in the absence of trypsin (Fig. 4*A*). Viral infectivity of the supernatants in SARS-CoV-infected cells cultured with or without trypsin also indicated that trypsin treatment enhanced viral growth by ≈100-fold (Fig. 4*B*). We also examined growth kinetics of SARS-CoV in the presence of low-concentration proteases (62.5 μg/ml trypsin, 125 μg/ml elastase) that do not detach cells from plates during culture for 42 h. It was also shown that protease enhanced virus replication (Fig. 4*C*) with remarkable fusion formation (Fig. 4*D*). All of these results strongly suggest that the virus spreads efficiently from cell to cell in the presence of trypsin, which cleaves S to S1 and S2 to allow cell entry of SARS-CoV via the cell surface.

We next examined the effects on low moi by other proteases that facilitate SARS-CoV entry from VeroE6 cell surface. As shown in Fig. 5, all of the proteases that produce S2 (Fig. 1*B*) and that induce cell-cell fusion enhanced virus spread. In contrast, those proteases that did not generate S2 and that did not induce cell-cell fusion failed to enhance the infection. These observations suggest that proteases that facilitate SARS-CoV entry from the cell surface support efficient SARS-CoV infection. Thus, protease is likely to be responsible for the high multiplication of

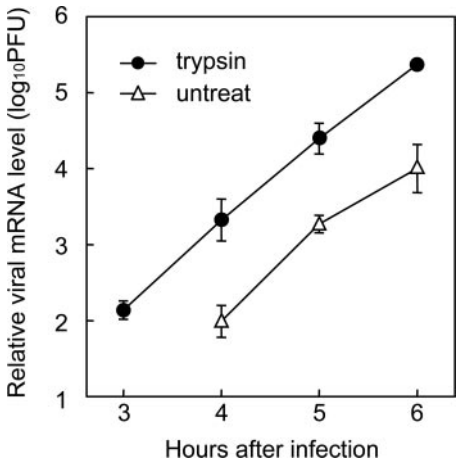

Fig. 3. Kinetics of mRNA9 synthesis after treatment of trypsin. VeroE6 cells were treated with Baf, infected with SARS-CoV, and treated with 200 μg/ml trypsin as described in the legend to Fig. 2*A*. The amount of mRNA9 synthesized was monitored by real-time PCR at 3–6 h after inoculation. VeroE6 cells without any treatment were also infected as a control (untreated). Relative viral mRNA level is displayed by virus infectivity (pfu) calculated from the calibration line shown in Fig. 2*C*.

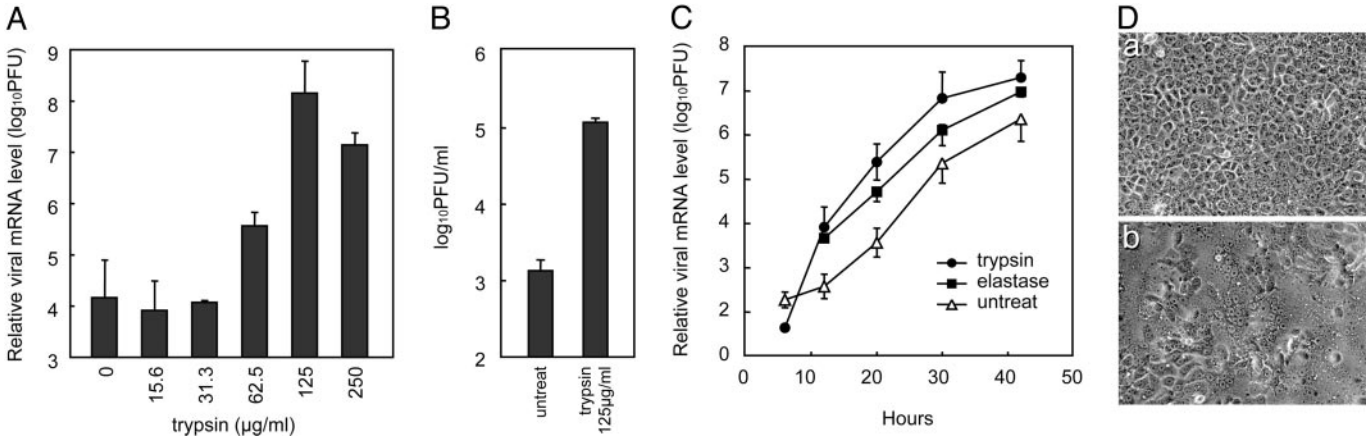

Fig. 4. Enhancement of SARS-CoV infection by proteases. (*A*) Effect of trypsin on virus replication in VeroE6 cells. Approximately 1×10^5 VeroE6 cells cultured in 24-well plates were infected with 10 pfu of SARS-CoV (moi = 0.0001) and cultured in the presence of varied trypsin concentrations. Viral replication was estimated at 20 h after infection by the amount of mRNA9, as measured by real-time PCR. (*B*) Viral infectivity was examined by plaque assay after 20-h incubation in the presence or absence of trypsin (125 μg/ml). (*C*) Viral growth kinetics after infection was examined in cultures in the presence or absence of trypsin (62.5 μg/ml) or elastase (125 μg/ml) by real-time PCR. Cells were harvested from 4 to 42 h after infection at intervals and the level of mRNA9 was monitored. Relative viral mRNA level is displayed by virus infectivity (pfu) calculated from a calibration line (*A*–*C*). (*D*) Cytopathic changes of virus-infected cells cultured in the presence (*b*) or absence (*a*) of trypsin (125 μg/ml) for 42 h are shown.

SARS-CoV in the major target organs of SARS, such as the lungs and bronchus, where various proteases are produced (e.g., by inflammatory cells), as well as in the intestines, where a number of proteases are physiologically secreted.

One of the major proteases produced by inflammatory cells in the lungs is an elastase produced by neutrophils (12), the accumulation of which was reported in the lungs of SARS patients (13). The level of elastase in bronchoalveolar lavage fluids was reported to reach levels as high as 700 μg/ml (12). Accordingly, we determined whether this protease has the potential to enhance SARS-CoV infection in a fashion similar to that of trypsin or thermolysin. Elastase was revealed to enhance SARS-CoV infection in cultured VeroE6 cells in terms of S protein cleavage (Fig. 1*B*), its cell-surface-mediated entry pathway (Fig. 2*A*), and its growth enhancement ability after low moi

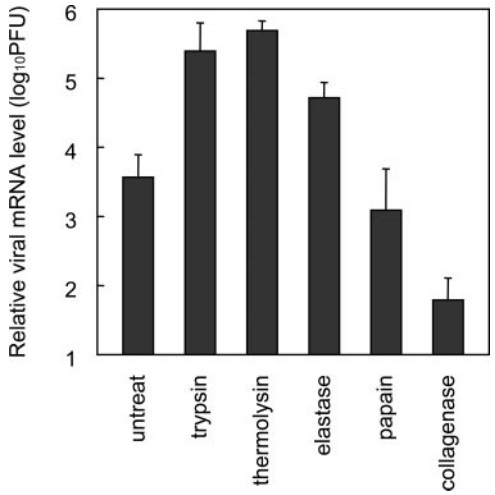

Fig. 5. Effect of various proteases on virus replication in VeroE6 cells. VeroE6 cells in 24-well plates were infected as described in Fig. 4 and cultured in the presence of trypsin (62.5 μg/ml), thermolysin (12.5 μg/ml), elastase (125 μg/ml), papain (0.037 unit/ml), or collagenase (200 μg/ml). At 20 h after infection, the amounts of mRNA9 were measured by real-time PCR. Relative viral mRNA level is displayed by virus infectivity (pfu) calculated from the calibration line.

(Figs. 4*C* and 5). These results strongly suggest that SARS-CoV replication can be enhanced in the lungs by elastase.

Discussion

The SARS-CoV gene and viral antigens were found in a number of organs, such as the liver, cerebrum, pancreas, and kidneys, as well as in such major target organs as the bronchus, lungs, and intestines (14–17), with the latter showing drastic tissue damage by SARS-CoV infection, whereas the other organs were not so severely affected. Although the pathogenic mechanism of SARS has not been elucidated, the present study suggests that proteases secreted in major target organs play an important role in the high multiplication of virus in those organs, which, in turn, results in severe tissue damage. An initial infection by SARS-CoV in pneumocytes via its receptor ACE2 (18), the endosomal pathway, could induce inflammation that generates a variety of proteases such as elastase. Once those proteases are present in the lungs, they may mediate an ensuing robust infection, which may result in enhanced replication of SARS-CoV in the lungs. Although lung damage is postulated to be mediated by cytokines by a so-called cytokine storm (14, 16), higher virus multiplication could also contribute to the cytokine storm by killing a large number of infected cells. A variety of proteases secreted in the small intestines, another major target organ of SARS-CoV, could also be responsible for the high growth of SARS-CoV in these tissues, which could result in a high rate of diarrhea in SARS patients (19, 20).

Protease-mediated enhancement of infection is known for orthomyxovirus and paramyxovirus infections (21–24), in which their envelope glycoprotein is not fully cleaved in *de novo* synthesized cells, and thus the virus particles produced contain partially cleaved or uncleaved glycoprotein. Those glycoproteins on virions are cleaved after treatment with protease, which results in the enhancement of infectivity. Thus, trypsin affects directly virons and increases the infectivity of those viruses. However, enhancement of SARS-CoV infection by trypsin or other proteases is mediated by another mechanism. Although trypsin treatment *in vitro* induces cleavage of the S protein on virions, such treatment never enhances SARS-CoV infectivity but reduces it to 1/10–1/100 of the original titer. Only S protein bound to its receptor ACE2 and cleaved by proteases could obtain fusion activity. Based on this idea, it is most likely that

binding of S protein to ACE2 induces conformational changes of the S, which is inevitable to be correctly processed for fusion activity by proteases. In other words, proteases can successfully induce the fusion activity of S protein only after S-ACE2 binding. Alternatively, protease treatment of virions digests out the S1 portion important for ACE2 binding, resulting in a loss of infectivity, whereas S2 alone is sufficient for fusion after binding to its receptor despite loss of the S1 fragment.

Why is the infection via the endosomal pathway not as efficient as direct infection from the cell surface? Throughout our examinations, replication deriving from the cell surface pathway began 1 h ahead of that via the endosomal pathway. We assume that a virus needs ≈1 h for trafficking from the cell surface where virion binds to ACE2 to the endosome. When cells are infected with an extremely low moi, a condition that occurs in natural infection, a 100- to 1,000-fold higher rate of infection was observed in the presence of proteases. Thus a 10-fold difference at 6 h after inoculation could result in a 1,000-fold difference, provided that one cycle of SARS-CoV replication is ≈6 h (25) and three rounds of infection take place within 20 h.

The present studies suggest that coinfection of SARS-CoV with some other non- or low-pathogenic respiratory agents, such as *Chlamydia*, mycoplasma, or bacteria, results in severe lung disease, which is attributed to the proteases produced by the infection with those non-SARS-CoV agents, as has been shown by the enhancement of respiratory diseases caused by influenza virus coinfected with nonpathogenic bacteria (26, 27). Studies are in progress to see whether coinfection exacerbates pneumonia in mice infected with SARS-CoV.

We thank Miyuki Kawase for excellent technical assistance throughout the experiments, John Ziebuhr (University of Würzburg, Würzburg, Germany) for providing SARS-CoV Frankfurt-1, and Judith White (University of Virginia, Charlottesville) for valuable comments on this work. We also thank the colleagues of our institute, especially Shuetsu Fukushi, Keiko Nakagaki, Kohji Ishii, and Yasuko Yokota, for valuable discussions and encouragement throughout the research. This work was supported by Ministry of Education, Culture, Sports, Science, and Technology Grant 16017308 and Ministry of Health, Labor, and Welfare Grant H16-Shinkoh-9.

1. Ksiazek, T .G., Erdman, D., Goldsmith, C., Zaki, S. R., Peret, T., Emery, S., Tong, S., Urbani, C., Comer, J. A., Lim, W., *et al.* (2003) *N. Engl. J. Med.* **348,** 1953–1966.
2. Drosten, C., Gunther, S., Preiser, W., Van Der Werf, S., Brodt, H. R., Becker, S., Rabenau, H., Panning, M., Kolesnikowa, L., Fouchier, R. A., *et al.* (2003) *N. Engl. J. Med.* **348,** 1967–1976.
3. Marra, M. A., Jones, S. J., Astell, C. R., Holt, R. A., Brooks-Wilson, A., Buttefield, Y. S., Khattra, J., Asano, J. K., Barber, S. A., Chan, S. Y., *et al.* (2003) *Science* **300,** 1399–1404.
4. Rota, P. A., Oberste, M. S., Monroe, S. S., Nix, W. A., Campagnoli, R., Icenogle, J. P., Penaranda, S., Bankamp, B., Maher, K., Chen, M. H., *et al.* (2003) *Science* **300,** 1394–1399.
5. The Chinese SARS Molecular Epidemiology Consortium (2004) *Science* **303,** 1666–1669.
6. Peiris, J. S., Guan, Y. & Yuen, K. Y. (2005) *Nat. Med.* **10,** 588–597.
7. Lai, M. M. C. & Cavanagh, D. (1997) *Adv. Virus Res.* **48,** 1–100.
8. Tyrell, D. A. J., Almeida, J. D., Berry, D. M., Cunningham, C. H., Hamre, D., Hofstad, M. S., Mallucci, L. & McIntosh, K. (1968) *Nature* **220,** 650.
9. Gallagher, T. M., Escarmis, C. & Buchmeier, M. J. (1991) *J. Virol.* **65,** 1916–1928.
10. Simmons, G., Reeves, J. D., Rennekamp, A. J., Amberg, S. M., Piefer, A. J. & Bates, P. (2004) *Proc. Natl. Acad. Sci. USA* **101,** 4240–4245.
11. Matsuyama, S. & Taguchi, F. (2000) *Virology* **273,** 80–89.
12. Kawabata, K., Haio, T. & Matsuoka, S. (2002) *Eur. J. Pharmacol.* **451,** 1–10.
13. Wong, C. K., Lam, C. W., Wu, A. K., Ip, W. K., Lee, N. L., Chan, I. H., Lit, L. C., Hui, D. S., Cha, M. H., Chung, S. S., *et al.* (2004) *Clin. Exp. Immunol.* **136,** 95–103.
14. Nicholls, J. M., Poon, L. L., Lee, K. C., Ng, W. F., Lai, S. T., Leung, C. Y., Chu, C. M., Hui, P. K., Mak, K. L., Lim, W., *et al.* (2003) *Lancet* **361,** 1773–1778.
15. Peiris, J. S. M., Lai, S. T., Poon, L. L. M., Guan, Y., Yam, L. Y. C., Lim, W., Nicholls, J., Yee, W. K. S., Yan, W. W., Cheung, M. T., *et al.* (2003) *Lancet* **361,** 1767–1772.
16. Tse, G. M., To, K. F., Chan, P. K., Lo, A. W., Ng, K. C., Wu, A., Lee, N., Wong, H. K., Mac, S. M., Chan, K. F., *et al.* (2004) *J. Clin. Pathol.* **57,** 260–265.
17. To, K. F. & Lo, A. W. (2004) *J. Pathol.* **203,** 740–743.
18. Li, W., Moore, M. H., Vasilieva, N., Sui, J., Wong, S. K., Berne, M. A., Somasundaran, M., Sullivan, J. L., Luzuriaga, K., Greenough, T. C., *et al.* (2003) *Nature* **426,** 450–454.
19. Zhan, J., Chen, W., Li, C., Wu, W., Li .J., Jiang, S., Wang, J., Zeng, Z., Huang, Z. & Huang, H. (2003) *Clin. Med. J.* **116,** 1265–1266.
20. Leung, W. K., To, K. F., Chan, P. K., Chan, H. L., Wu, A. K., Lee, N., Yuen, K. Y. & Sung, J. J. (2003) *Gastroenterology* **125,** 1011–1017.
21. Rott, R., Orlich, M. & Blodorn, J. (1975) *Virology* **68,** 426–439.
22. Nagai, Y., Klenk, H. D. & Rott, R. (1976) *Virology* **72,** 494–508.
23. Ohuchi, M. & Homma, M. (1976) *J. Virol.* **18,** 1147–1150.
24. Tashiro, M., Yokogoshi, Y., Tomita, K., Seto, J. T., Rott, R. & Hido, H. (1992) *J. Virol.* **72,** 11–16.
25. Ng, M.-L., Tan, S.-H., See, E. E., Ooi, E. E. & Ling, A. E. (2003) *J. Gen. Virol.* **84,** 3291–3303.
26. Tashiro, M., Ciborowski, P., Klenk, H.-D., Pulverer, G. & Rott, R. (1987) *Nature (London)* **325,** 536–537.
27. Kishida, N., Sakoda, Y., Eto, M., Sunaga, Y. & Kida, H. (2004) *Arch. Virol.* **149,** 2095–2140.